Stem Cells Translational Medicine, 2025, **14**, szae101
https://doi.org/10.1093/stcltm/szae101
Advance access publication 26 March 2025
Original Research

TGFBR3 dependent mechanism of TGFB2 in smooth muscle cell differentiation and implications for TGFB2-related aortic aneurysm

Ying Tang[1,2], Jiaxi Cheng[1], Cynthia Huang[1], Ping Qiu[1], Jingxin Li[1,2], Yuqing Eugene Chen[1,3], Dogukan Mizrak[1,*], Bo Yang[1,*]

[1]Department of Cardiac Surgery, University of Michigan, Ann Arbor, MI 48109, United States
[2]Second Xiangya Hospital, Central South University, Changsha 410011, China
[3]Department of Internal Medicine, University of Michigan, Ann Arbor, MI 48109, United States

[*]Corresponding authors. Dogukan Mizrak, Department of Cardiac Surgery, University of Michigan, Ann Arbor, MI 48109, USA. E-mail: dmizrak@med.umich.edu; Bo Yang, Department of Cardiac Surgery, University of Michigan, Ann Arbor, MI 48109, USA. E-mail: boya@med.umich.edu.

Introduction: Pathogenic variants in canonical transforming growth factor β (TGFβ) signaling genes predispose patients to thoracic aortic aneurysm and dissection (TAAD), predominantly in aortic root. Although TAAD pathogenesis associated with TGFβ receptor defects is well characterized, distinct and redundant mechanisms of TGFβ isoforms in TAAD incidence and severity remain elusive.

Objective: Here we examined the biological role of TGFB2 in smooth muscle cell (SMC) differentiation and investigated how TGFB2 defects can lead to regional TAAD manifestations.

Methods: To characterize the role of TGFB2 in SMC differentiation and function, we employed human-induced pluripotent stem cell (hiPSC)-derived SMC differentiation, CRISPR/Cas9 gene editing, three-dimensional SMC constructs, and human aortic tissue samples.

Results: Despite the similar effects of different TGFβ isoforms on hiPSC-derived SMC differentiation, siRNA experiments revealed that TGFB2 distinctively displays TGFBR3 dependence for signal transduction, an understudied TGFβ receptor in TAAD. Molecular evaluation of different thoracic aorta regions suggested TGFB2 and TGFBR3 enrichment in the aortic root tunica media. *TGFB2* haploinsufficiency ($TGFB2^{KO/+}$) and TGFB2 neutralization impaired the differentiation of second heart field-derived SMCs. $TGFBR3^{KO/KO}$ prevented the molecular rescue of $TGFB2^{KO/+}$ by TGFB2 supplementation indicating the involvement of TGFBR3 in TGFB2-mediated SMC differentiation. Lastly, a missense *TGFB2* variant ($TGFB2^{G276R/+}$) caused mechanical defects in SMC tissue ring constructs that were rescued by TGFB2 supplementation or genetic correction.

Conclusion: Our data suggests the distinct regulation and action of TGFB2 in SMCs populating the aortic root, while redundant activities of TGFβ isoforms provide implications about the milder TAAD aggressiveness of pathogenic TGFB2 variants.

Key words: TGFβ signaling; thoracic aortic aneurysm; smooth muscle cell; CRISPR/Cas9 gene editing; human induced pluripotent stem cells.

Received: 27 June 2024; Accepted: 18 December 2024.

Graphical abstract

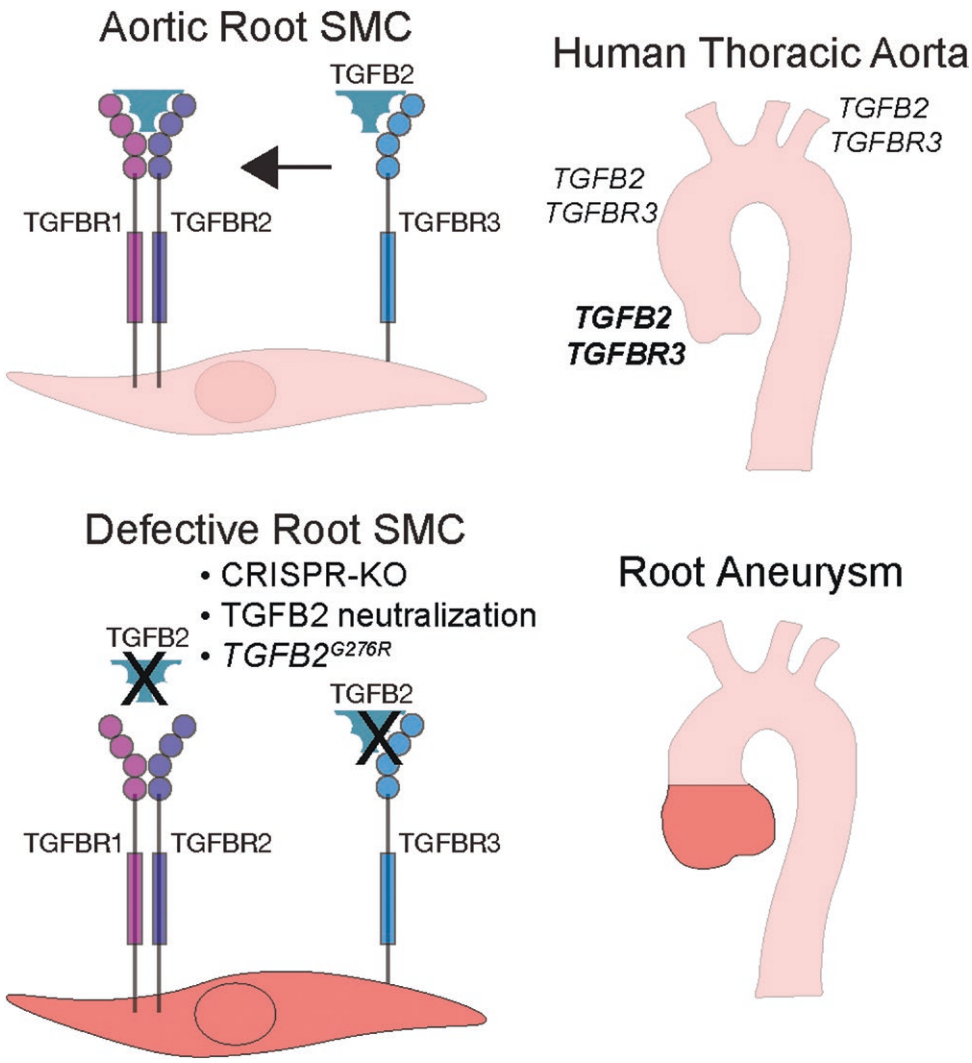

Significance statement

Genetic defects in transforming growth factor β (TGFβ) signaling genes predispose patients to thoracic aortic aneurysm and dissection (TAAD), predominantly in aortic root. Although canonical TGFβ receptors have been extensively studied in the TAAD field due to their central role in TGFβ signaling, the molecular link between different TGFβ isoforms and TAAD is not fully understood. Using hiPSC modeling, our data suggest TGFBR3-dependent mechanism of TGFB2 in smooth muscle cell differentiation implicating the nonredundant role of TGFB2 in aortic SMC physiology while compensatory activities of TGFβ isoforms provide implications about the milder TAAD aggressiveness associated with their pathogenic variants.

Introduction

Genetic predisposition is a risk factor for thoracic aortic aneurysm and dissection (TAAD), which causes significant morbidity and mortality.[1-3] Inactivating pathogenic variants in canonical transforming growth factor β (TGFβ) signaling genes (*TGFBR1*, *TGFBR2*, *SMAD3*, *SMAD2*, *TGFB2,* and *TGFB3*) predispose patients to TAAD in the aortic root, also known as Loeys-Dietz Syndrome (LDS).[2,4-8] In fact, TGFβ signaling dysregulation is observed in other syndromic TAAD forms including Marfan Syndrome.[9,10] TGFβ signaling is essential for vascular smooth muscle cell (SMC) differentiation and aortic wall integrity.[6,7,11-14] An LDS mouse model and our human induced pluripotent stem cell (hiPSC) disease modeling studies demonstrated that mutations in *TGFBR1* disrupt SMCs derived from second heart field cardiovascular progenitor cells (CPC-SMCs) in a lineage-specific manner, sparing neural crest stem cell lineage SMCs (NCSC-SMCs).[15,16] Likewise, *Tgfbr2* deletion in postnatal SMCs causes aneurysms both in aortic root and ascending aorta in mouse models.[17] As aortic root is mostly populated with CPC-SMCs, these findings informed the etiology of aortic root aneurysms in LDS patients.

TGFβ signaling is initiated when a TGFβ ligand engages type II and type I TGFβ receptors (TGFBR2 and TGFBR1). In the canonical signaling, the TGFβ receptor complex phosphorylates the regulatory SMADs; SMAD3 (Mothers against decapentaplegic homolog 3) and SMAD2 (Mothers

against decapentaplegic homolog 2), to alter gene transcription. Non-canonical TGFβ signaling refers to the activation of other downstream effectors such as ERK (extracellular signal-regulated kinase), p38 mitogen-activated protein kinase, and AKT (Protein kinase B) by the receptor complex.[18] There are 3 TGFβ isoforms (TGFB1, TGFB2, and TGFB3) regulating TGFβ receptor signaling and their knockout mice phenotypes show both common and non-overlapping features.[19] *Tgfb2* knockout mice display perinatal mortality with congenital heart, lung, and outflow tract defects, skeletal malformations, and cleft palates while *Tgfb1* null mice have widespread immune system defects with an inflammatory phenotype.[20-23] Similar to *Tgfb2* knockout mice, *Tgfb3* null mice also have cleft palates and lung defects; however, aortic defects observed in *Tgfb2* knockout mice are minimal.[24-28] *Tgfb2* and *Tgfb3* expression patterns in the developing cardiovascular system show significant overlap with enrichment in arterial tunica media and adventitia, while *Tgfb1* expression appears more restricted to intima.[29] These observations suggest nonredundant activity of TGFB2 in cardiovascular development that invites further exploration within TAAD context.

Despite the association of several TGFβ signaling genes in human TAAD, there are also differences between their phenotypic manifestations. The pathogenic variants in *TGFBR1*, *TGFBR2*, and *SMAD3* have similar aortic phenotypes with early disease onsets. Pathogenic *TGFB2* or *TGFB3* variants are often less penetrant in families and have milder aortic phenotypes,[6,7,30,31] while *TGFB1* variants are not strongly associated with TAAD formation.[32] In addition, *TGFB2* variants can cause Kawasaki disease often characterized with coronary artery aneurysm, ischemic heart disease, and sudden cardiac death implying pervasive effects of *TGFB2* in the human cardiovascular system.[33] Here we investigated the distinct mode of action of TGFB2 on SMC differentiation using both monolayer and 3D tissue ring cultures. Through the utilization of hiPSC-derived SMCs, SMC tissue constructs, human aorta samples, and CRISPR/Cas9 gene editing, our data have implications about the unique contribution of TGFB2 defects to aortic root aneurysm formation.

Materials and methods

Additional materials and methods, and the detailed list of reagents, primers, and primary and secondary antibodies are available in Tables S1 and S2.

Study approval

All experiments were performed according to the protocols approved by the Institutional Review Board at the University of Michigan (HUM00054585 and HUM00052866).

Human iPSCs generation and CRISPR/Cas9 gene editing

Human induced pluripotent stem cells were generated as described previously.[16,34] For CRISPR/Cas9 gene editing, single guide RNA (sgRNA, IDT) with the sequence *5'-CCACTAGGAAAAAAAACAGT-3'* was used to target the upstream of *TGFB2 c.826G*. To form the ribonucleoprotein (RNP) complex, 10 μg S.p. HiFi Cas9 Nuclease V3 (IDT) and 7.5 μg of sgRNA were first incubated for 10 minutes at room temperature. Then, 10 μg of designed single-strand oligo donor DNAs (ssODNs, IDT) were added to the mixture. About 2 × 10^6 hiPSCs were electroporated with the RNP mixture using Celetrix electroporation system (Celetrix, Manassas, VA, USA) with the program: V set (630V); T set (30 ms); P num (1N); P int (1 ms). Transfected hiPSCs were seeded on Corning GFR Matrigel-coated 35mm dishes in TesRE8 medium (Catalog No. 05990, STEMCELL Technologies) and cultured until the formation of visible clones. A heterozygous knockout clone with a 7 base-pair deletion causing a premature stop codon in *TGFB2* gene was selected for further experiments. Two ssODNs were designed to induce the *TGFB2 c.826G>A* (p. Gly276Arg) mutation in healthy male hiPSCs or to correct *TGFB2 c.826G>A* (p. Gly276Arg) variant in hiPSCs derived from a male patient. A heterozygous clone with *TGFB2 c.826G>A* mutation, and 2 independent patient correction clones were selected for subsequent experiments. The *TGFB2* heterozygous knockout clone was also used to perform *TGFBR3* gene editing. SgRNA with the sequence *5'-ACACTATTCCTCCTGAGCTA-3'* was used to target *TGFBR3* gene. A homozygous clone with 14 base-pair deletion and a homozygous clone with 1 base-pair insertion, which caused premature stop codons in *TGFBR3* gene, were selected for further experiments. The Sanger sequencing primers used in the study are listed in Table S1.

Generation of SMCs from human iPSCs

Differentiation of hiPSC to CPC-SMCs and NCSC-SMCs was performed as described previously.[16,34-38] For CPC-SMC differentiation, hiPSCs were seeded on Matrigel-coated plates at a density of 3 × 10^4 cells/cm^2 in TesRE8 medium with 10 μmol/L Y27632 (Biogems), and then incubated in CPC differentiation medium (DMEM/F12 (Gibco), B27 (without vitamin A, Gibco), 25 ng/mL BMP4 (PeproTech), 8 μmol/L CHIR99021 (Biogems), 50 μg/mL ascorbic acid (Sigma), 400 μmol/L 1-thioglycerol (Sigma), and 1% penicillin-streptomycin (Gibco)) for 3 days. The resulting CPCs were seeded at a density of 1.5 × 10^4 cells/cm^2 and incubated for 7 days in CPC-SMC basic medium (DMEM/F12, B27, 1% penicillin-streptomycin, 400 μmol/L 1-thioglycerol, 10 ng/mL PDGFBB (PeproTech)) with either vehicle (0.1% BSA with no TGFβ ligand), 2 ng/mL active TGFB1 (PeproTech), 2 ng/mL active TGFB2 (PeproTech) or 2 ng/mL full-length TGFB2 (Acro). For NCSC-SMC differentiation, hiPSCs were seeded on Matrigel-coated dishes at a density of 2 × 10^4 cells/cm^2 in TesRE8 medium with 10 μmol/L Y27632. After reaching nearly 50% confluency, they were incubated in NCSC differentiation medium (DMEM/F12, 1 × N2 supplement [Gibco], 0.1% BSA [Sigma], 1% penicillin-streptomycin plus 10 μmol/L SB4315421 [Biogems], and 1 μmol/L LDN193189 [Biogems]) for 6 days. From day 2 to day 6, 3 μmol/L CHIR99021 was added to the medium. The resulting NCSCs were seeded at a density of 8 × 10^4 cells/cm^2 in NCSC medium with 10 μmol/L Y27632. One day later, the cells were differentiated using NCSC-SMC basic medium (DMEM/F12, 20% knockout serum replacement (Gibco), 1% penicillin-streptomycin) with either vehicle (0.1%BSA with no TGFβ ligand), 2 ng/mL active TGFB1 or 2 ng/mL active TGFB2 for 8 days.

Tissue ring assays and analysis

Tissue rings with a diameter of 2 mm were prepared as described previously.[16,34,39] Briefly, on day 5 of the CPC-SMC differentiation, SMCs were harvested using Accutase (Gibco) and seeded on Matrigel-coated 100 mm dishes with a density

of 2.5×10^4 cells/cm^2. The cells were cultured in DMEM/F12 with 10% FBS. The cells were harvested when they reached 80%-90% confluence (3-4 days) and seeded on agarose molds at a density of 1×10^6 cells/well in DMEM/F12 with 10% FBS. The tissue ring culture medium (DMEM (high glucose), 20% FBS, 1% penicillin-streptomycin, 1 ng/mL TGFB1, and supplemented with proline (50 μg/mL), glycine (50 μg/mL), alanine (20 μg/mL), $CuSO_4$ (3 ng/mL), and ascorbic acid (50 μg/mL) was applied on the second day of the tissue ring culture. Medium was replaced every 2 days. The rings were harvested on day 14 for subsequent analysis. For uniaxial tensile tests, both sides of each ring were measured to calculate its thickness. The length and width of the rings were also measured and recorded. Mechanical tests were performed using a uniaxial test machine (TA Instruments RSA-G2). The tissue rings were stretched with custom rectangular loops threaded through each ring and then clamped into standard thin film fixtures (TA Instruments). The samples were then pulled to failure at a speed of 10 mm/minute. For each ring, the force (N) and strain (%) were recorded throughout the test. Two mechanical parameters were calculated from the acquired data using MATLAB software: ultimate tensile strain (maximal tension divided by a cross-sectional area of tissue during the recording [MPa = N/mm^2]), ultimate strain (elongated length at the maximal tension divided by the initial length [%]). Active human TGFB2 protein levels were assessed in tissue ring lysates using a TGFB2 enzyme-linked immunosorbent assay (ELISA) kit (Catalog No. DB250, R&D Systems). Active TGFB2 levels were measured without sample acidification as described previously.[40,41] Active TGFB2 concentration in each tissue ring was normalized to total protein concentration. The immunofluorescence stainings were performed on CPC-SMC tissue rings generated in independent differentiation batches. Paraffin-embedded tissue rings were sectioned into 5 μm slices. After deparaffinization, rehydration, permeabilization, and heat antigen retrieval, the sections were blocked with 5% BSA for 1 hour at room temperature and then incubated with Myosin heavy chain 11 (Catalog No. ab133567, 1:100, Abcam) primary antibody in 1% BSA overnight at 4°C. Alexa Fluor 594 Donkey Anti-Rabbit IgG (Catalog No. 711585152, 1:500, Jackson Immuno Research) was used as the secondary antibody. The sections were counterstained with DAPI. Images were taken using BZ-X800 Keyence microscope. MYH11 staining intensity was quantified using Image J.[42] The cell density of each ring was determined by DAPI staining and quantified using Image J.

Statistics

All quantitative data were presented as mean ± standard deviation with at least 3 biological replicates. We conducted a Shapiro-Wilk normality test prior to all analysis. When analyzing >2 groups that were not normally distributed or when analyzing >2 groups with <6 biological replicates, we performed Kruskal-Wallis test with Dunn's multiple comparisons test. When analyzing >2 groups that were normally distributed ($n = 6$), we tested for equal variance using the Brown-Forsythe test. If the standard deviations were not significantly different, we performed 1-way analysis of variance (ANOVA) analysis with Dunnett's multiple comparisons test to compare the mean of each column with the mean of a control column. If the standard deviations were significantly different, we performed 1-way ANOVA analysis with Dunnett's T3 multiple comparisons test to compare the mean of each column with the mean of a control column. When analyzing only 2 datasets that were not normally distributed ($n \geq 3$), we performed Mann-Whitney U test. When analyzing only 2 datasets that were normally distributed ($n \geq 3$), we used the unpaired t-test. If the variances were significantly different, we conducted the unpaired t-test with Welch's correction. The statistical analyses were performed using GraphPad Prism Software.

Results

TGFB1 and TGFB2 have similar effects on hiPSC-derived SMC differentiation

Human aortic root is populated with SMCs derived from second heart field cardiovascular progenitor cells (CPC-SMCs) and TGFB2 defects predispose patients to TAAs predominantly in the aortic root.[43-45] Among TGFβ isoforms, TGFB1 is typically used in monolayer SMC differentiation protocols. To compare the activity of TGFB1 and TGFB2, we treated CPC progenitor cells either with vehicle (no TGFβ ligand), 2 ng/mL biologically active recombinant TGFB1, or with 2 ng/mL biologically active recombinant TGFB2 during CPC-SMC differentiation. RT-qPCRs revealed a robust and comparable increase in SMC markers; *ACTA2* (actin alpha 2), *SM22α* (smooth muscle protein 22-alpha), *CNN1* (calponin 1), *MYOCD* (myocardin), *SMTN* (smoothelin), and *MYH11* (myosin heavy chain 11) in TGFB1 and TGFB2 treated CPC-SMCs compared to the vehicle (Figure 1A). We also measured the effects of full-length TGFB2 (FL-TGFB2) on CPC-SMC differentiation as a previous report suggested a lower activation threshold for FL-TGFB2.[46] However, FL-TGFB2 treatment failed to induce adequate expression of SMC markers in our culture conditions indicating the requirement of active TGFB2 for hiPSC-derived SMC marker expression (Figure 1B).

We also assayed the protein levels after CPC-SMC differentiation in active TGFB1 or active TGFB2 by immunoblots. Western blots revealed that both TGFB1 and TGFB2 treatments significantly increased SMC marker levels in CPC-SMCs (Figure 1C). The marker levels were similar between TGFB1 and TGFB2 treated CPC-SMCs further suggesting their redundant activity in CPC-SMC differentiation (Figure 1C). We also measured the activation of both canonical and non-canonical TGFβ signaling mediators in CPC-SMCs treated with either TGFB1 or TGFB2. To induce the phosphorylation of TGFβ downstream effectors, the differentiated CPC-SMCs were cultured in CPC-SMC basic medium for 24 hours, and then incubated with basic medium with or without 2 ng/mL active TGFB1 or TGFB2 for 1 hour prior to cell lysis. Consistent with the mRNA and protein quantifications, we observed similar levels of phosphorylated SMAD3 (pSMAD3), pSMAD2, pERK, and pAKT in CPC-SMCs treated with either TGFB1 or TGFB2 (Figure 1D).

Next, we examined whether the redundant activities of TGFB1 and TGFB2 in SMC contractile gene expression were independent of SMC developmental origins. To do this, we differentiated hiPSCs to NCSC-SMCs through neural crest stem cell (NCSC) lineage. *MYH11* appeared to be the most sensitive gene in NCSC-SMCs to both TGFB1 and TGFB2 treatments (Figure S1A and B). Importantly, TGFB2-treated NCSC-SMCs had similar SMC marker expression compared to TGFB1-treated NCSC-SMCs suggesting their comparable

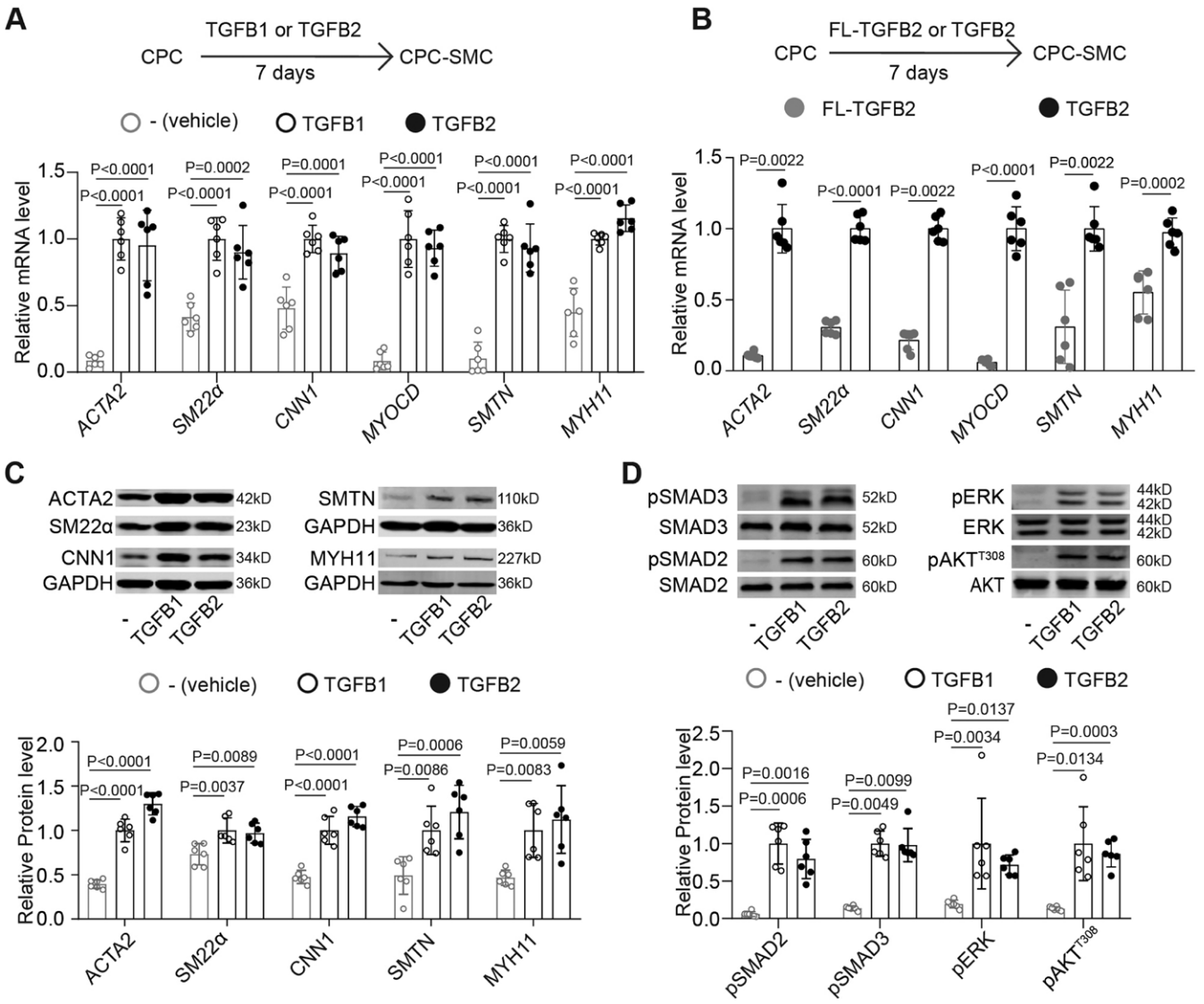

Figure 1. TGFB1 and TGFB2 have similar effects on hiPSC-derived SMC differentiation. (A) Relative expression of SMC markers in CPC-SMCs after differentiation with either 2 ng/mL active TGFB1, 2 ng/mL active TGFB2, or control (vehicle/no ligand). The average expression in the TGFB1-treated samples was set to 1. $n = 6$ biological replicates. (B) Relative expression of smooth muscle cell (SMC) markers in cardiovascular progenitor cells (CPC)-SMCs after differentiation with either 2 ng/mL active TGFB2 or 2 ng/mL full-length TGFB2 (FL-TGFB2). The average expression in the active TGFB2-treated samples was set to 1. $n = 6$ biological replicates. (C) Top: western blots of CPC-SMC protein extracts after differentiation with either active TGFB1 or TGFB2. Bottom: quantification of western blot data showing relative protein SMC marker levels in CPC-SMCs. $n = 6$ biological replicates. (D) Top: western blots of canonical and non-canonical TGFβ signaling mediators in CPC-SMCs after 1-hour stimulation with either active TGFB1, TGFB2, or vehicle. Bottom: quantification of western blot data for pSMAD2, pSMAD3, pERK, and pAKT (T308) after the stimulation. The average protein levels in the TGFB1 treated samples were set to 1. $n = 6$ biological replicates. 1-way analysis of variance (ANOVA) with multiple comparisons test.

activity in NCSC-SMC differentiation. Overall, these results suggest that TGFB1 and TGFB2 have indistinguishable effects on SMC marker expression in hiPSC-derived SMC differentiation.

TGFBR3 facilitates TGFB2 signaling transduction during SMC differentiation

Previous biophysical studies demonstrated that TGFB2 binds to TGFBR2 weakly and has the highest affinity to TGFBR3.[47] TGFBR3 does not have kinase activity and plays a part in TGFβ ligand presentation to TGFBR1-TGFBR2 complex with the kinase activity.[48] To investigate the contribution of TGFBR3 to SMC differentiation, we transfected CPC-SMCs with *TGFBR3*-siRNA and performed RT-qPCRs on CPC-SMCs differentiated with either active TGFB1 or TGFB2. *TGFBR3*-siRNA transfection reduced *TGFBR3* levels by nearly 50% in both conditions (Figure 2A and B). TGFB1-treated CPC-SMCs were insensitive to *TGFBR3* knockdown consistent with the low affinity of TGFB1 for TGFBR3 (Figure 2A). SMC markers including *MYOCD* and *SMTN* were reduced in TGFB2 treated CPC-SMCs upon *TGFBR3* knockdown (Figure 2B), suggesting that TGFB2 additionally depends on TGFBR3 to exert its effects on SMC differentiation.

To understand the signaling differences between TGFB1 and TGFB2, we transfected CPC-SMCs with *TGFBR1*-siRNA, *TGFBR3*-siRNA, or control siRNA for 2 days including the starvation period and treated the cells with either

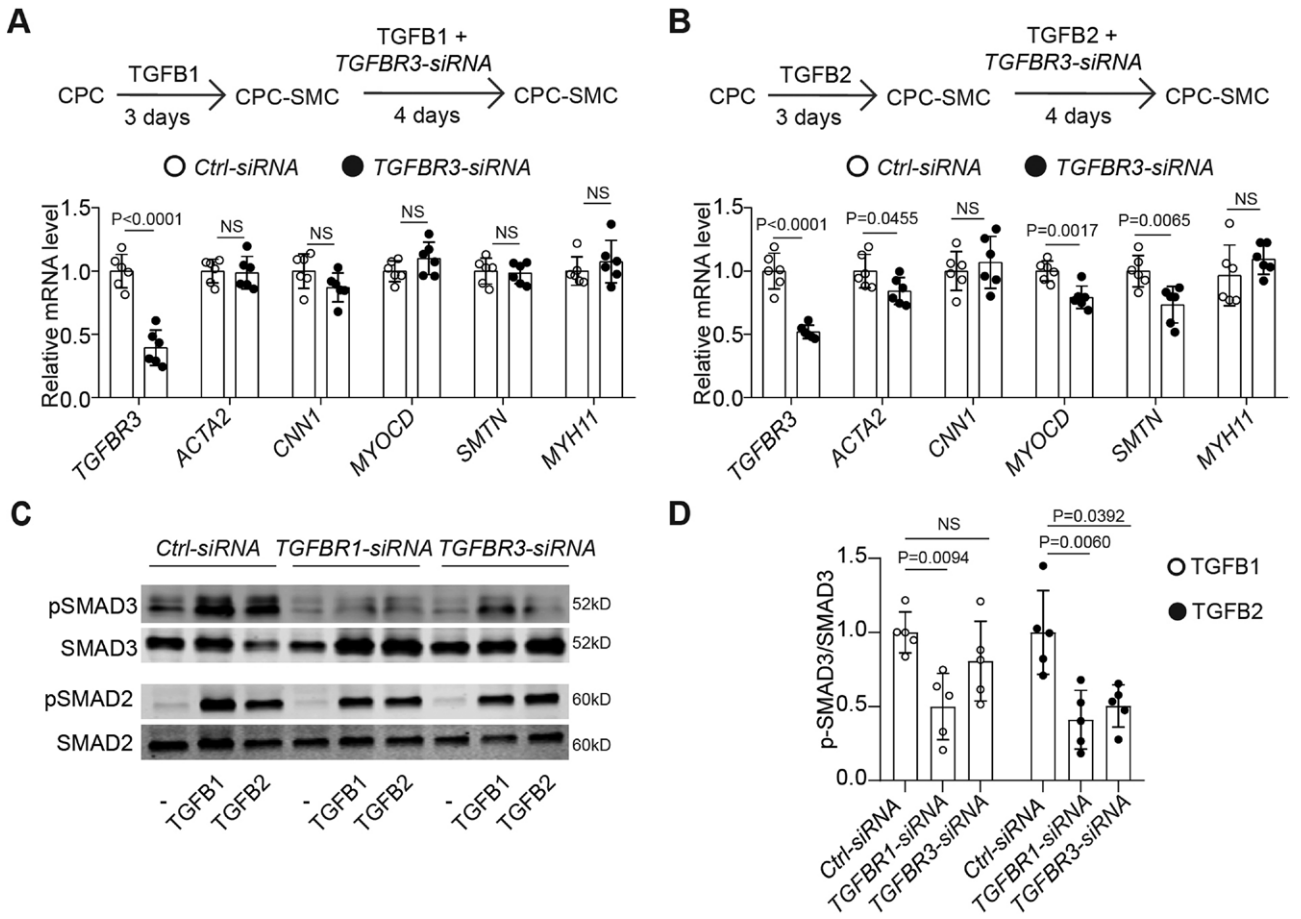

Figure 2. TGFBR3 facilitates TGFB2 signaling transduction during SMC differentiation. (A and B), Relative expression of SMC markers after TGFBR3-siRNA treatment. CPC-SMCs were transfected with 40nM TGFBR3-siRNA or control siRNA for 4 days during differentiation with either active TGFB1 or TGFB2. $n = 6$ biological replicates. ns: not significant; unpaired t-test or Mann-Whitney U test. (C) pSMAD3 and pSMAD2 western blots of CPC-SMC protein extracts stimulated with either active TGFB1, TGFB2 or vehicle for 1 hour. CPC-SMCs were transfected with 40 nM target siRNA (TGFBR1-siRNA or TGFBR3-siRNA) or control siRNA for 2 days. (D) Quantification of pSMAD3 western blot data. Each quantification was normalized to its vehicle control. The average levels in control siRNA-treated samples were set to 1. $n = 5$ biological replicates. ns: not significant; Kruskal-Wallis test with multiple comparisons test.

active TGFB1 or active TGFB2 for 1 hour prior to cell lysis (Figure S2A). As expected, control siRNA did not alter the induction profile for the regulatory SMADs; SMAD3 and SMAD2, and pSMAD3 level was significantly reduced in CPC-SMCs treated with either TGFB1 or TGFB2 upon *TGFBR1* knockdown (Figure 2C and D). In addition, *TGFBR3* knockdown did not alter pSMAD3 and pSMAD2 levels in CPC-SMCs treated with TGFB1. We observed a sharp decrease in pSMAD3 levels in CPC-SMCs treated with TGFB2 upon *TGFBR3* knockdown further suggesting that TGFB2 depends on TGFBR3 to activate SMAD3 (Figure 2C and D). pSMAD2 level was not sensitive to TGFBR3 knockdown in CPC-SMCs consistent with a previous report implicating the role of SMAD2 in NCSC-SMC differentiation.[49]

TGFB2 and *TGFBR3* expression show enrichment in the human aortic root

To understand the expression differences between different TGFβ signaling ligands and receptors, we next collected matching aortic root, ascending aorta, and aortic arch samples from non-aneurysmal patients, who were eventually disqualified for the heart transplant. To measure the gene expression changes, we used different thoracic aorta regions from both female and male patients, denoted as ♀ Donor-1, ♀ Donor-2, ♂ Donor-1, and ♂ Donor-2 (Figure 3A, Figure S2B). RT-qPCRs of tunica media showed *TGFB2* enrichment in the aortic root (Figure 3A). *TGFB1* expression also appeared higher in the aortic root, while *TGFB3* did not show a regional difference (Figure S2B). Among the TGFβ signaling receptors, the expression of core TGFβ receptors; *TGFBR2* and *TGFBR1*; did not show a regional expression bias while *TGFBR3* expression was higher in the aortic root (Figure 3B, Figure S2B). Next, we performed immunoblots on different thoracic aorta segments to confirm the enrichment of *TGFB2* and *TGFBR3* expression in the aortic root at the protein level (Figure 3C). The quantification of western blots validated higher TGFB2 and TGFBR3 levels in the aortic root tunica media (Figure 3D). These data suggest that there is a *TGFB2*-*TGFBR3* expression gradient in the human aorta peaking closer to the heart.

TGFB2 haploinsufficiency causes SMC differentiation defects

To characterize the molecular changes caused by TGFB2 defects in the hiPSC model, we introduced a monoallelic 7 base-pair deletion in human *TGFB2* gene (denoted as

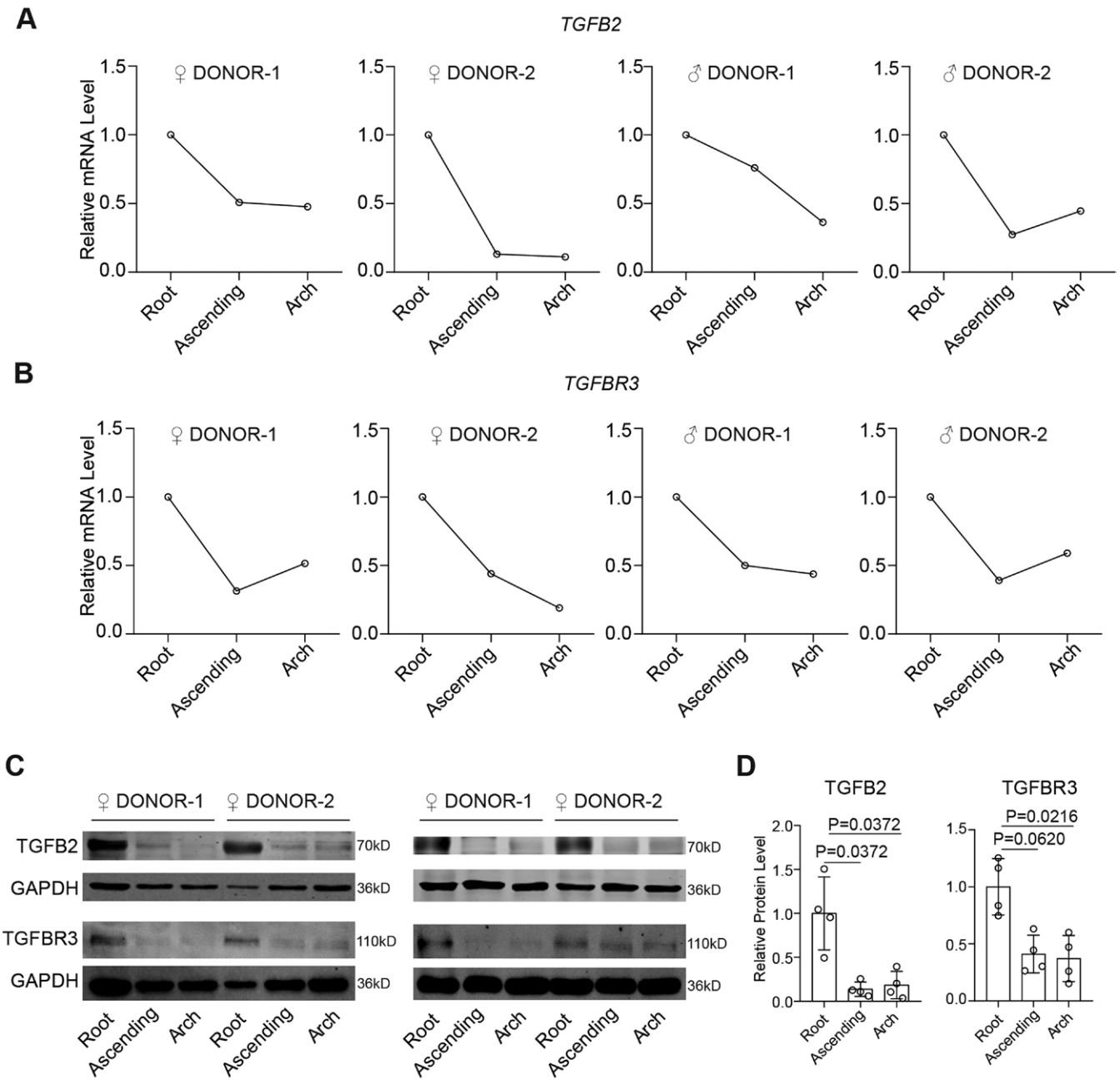

Figure 3. *TGFB2* and *TGFBR3* expression show enrichment in the human aortic root. (A) Relative expression of TGFB2 in aortic media of root, ascending, and arch samples. *TGFB2* expression level in each aortic root sample was set to 1. (B) Relative expression of TGFBR3 in aortic media of root, ascending, and arch samples. *TGFBR3* expression level in each aortic root sample was set to 1. (C) TGFB2 and TGFBR3 western blots of tunica media protein extracts from different thoracic aorta regions. (D) Quantification of western blot data showing TGFB2 and TGFBR3 enrichment in the aortic root media. $n = 4$ biological replicates. Kruskal-Wallis test with multiple comparisons test.

TGFB2$^{KO/+}$) using CRISPR/Cas9 gene editing. The deletion causes a premature stop codon prior to the active TGFB2 (cytokine) domain (Figure 4A). RT-qPCRs and western blots revealed a significant reduction in *TGFB2* mRNA and protein levels in heterozygous *TGFB2*$^{KO/+}$ CPC-SMCs (Figure 4B). To examine the molecular consequences of *TGFB2*^{KO}, we performed transwell co-culture assays. We seeded *TGFB2*$^{KO/+}$ CPCs in the top layer and co-cultured them with either *TGFB2*$^{KO/+}$ or *TGFB2*$^{+/+}$ CPCs for 6 days in CPC-SMC differentiation medium (Figure 4C). In addition, *TGFB2*$^{+/+}$ CPCs were co-cultured with *TGFB2*$^{+/+}$ CPCs as a control. The 0.4 μm pores allowed the passage of secreted factors between the hanging insert and the dish while preventing the migration of the cells (Figure 4C). On day 7 of differentiation, *TGFB2*$^{+/+}$ CPC-SMCs had higher expression of several SMC markers compared with *TGFB2*$^{KO/+}$ CPC-SMCs (Figure 4D). Interestingly, *TGFB2*$^{KO/+}$ CPC-SMCs co-cultured with *TGFB2*$^{+/+}$ CPC-SMCs had significantly higher expression of SMC markers including *MYH11* and *CNN1* suggesting that secreted factors from *TGFB2*$^{+/+}$ CPC-SMCs can improve SMC marker expression in *TGFB2*$^{KO/+}$ CPC-SMCs (Figure 4D).

To formally test whether TGFB2 is among the secreted factors that promote SMC marker expression, we supplemented *TGFB2*$^{KO/+}$ CPC-SMCs with either vehicle or

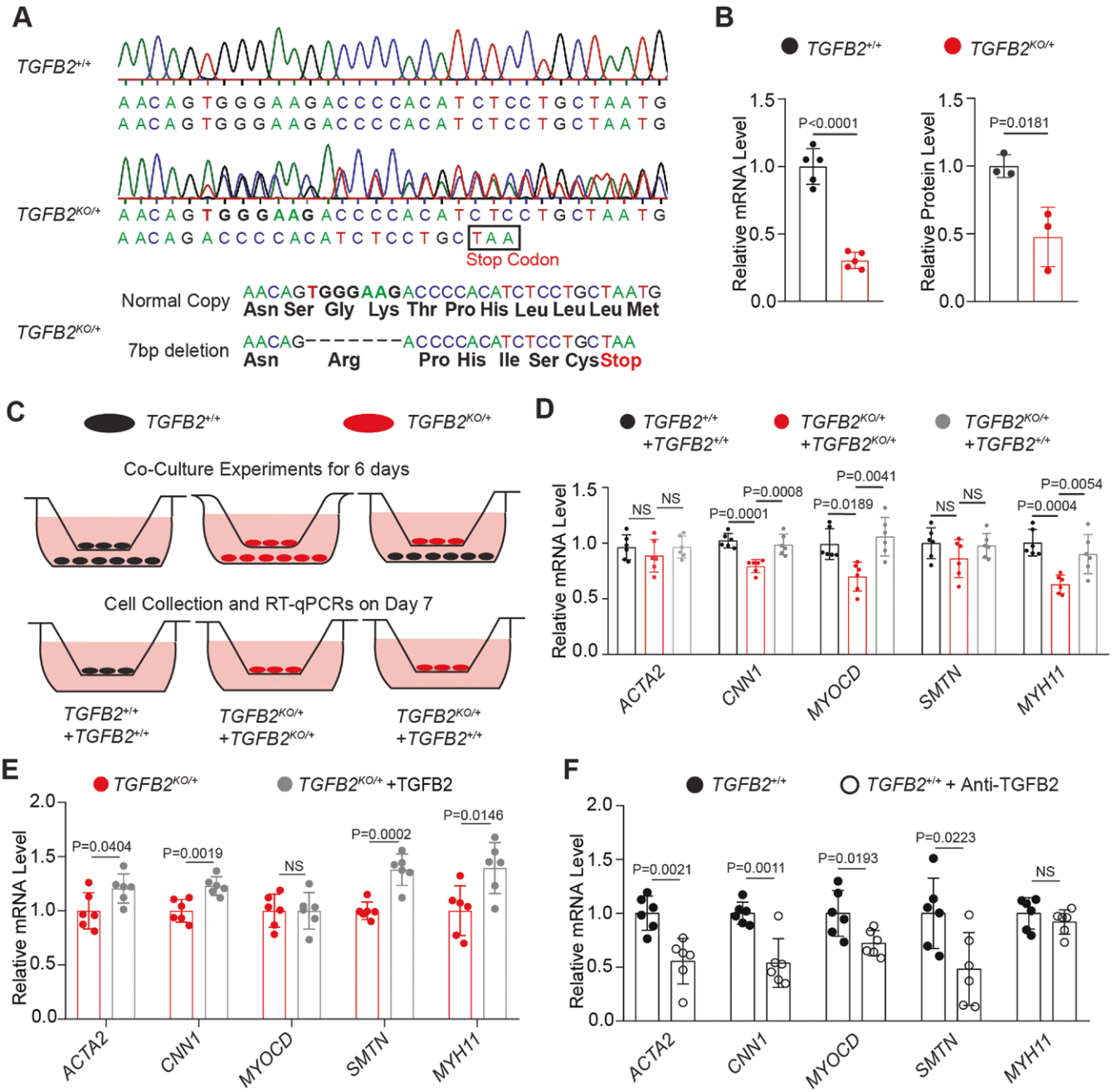

Figure 4. *TGFB2* haploinsufficiency causes SMC differentiation defects. (A) The Sanger sequencing results for $TGFB2^{+/+}$ and $TGFB2^{KO/+}$ showing the position of 7 base-pair deletion resulting in a premature stop codon in *TGFB2* gene. (B) Left: relative *TGFB2* expression in $TGFB2^{+/+}$ and $TGFB2^{KO/+}$ SMCs. $n = 6$ biological replicates. unpaired t-test. Right: relative TGFB2 protein levels in $TGFB2^{+/+}$ and $TGFB2^{KO/+}$ SMCs. $n = 3$ biological replicates; unpaired t-test. (C) Diagram showing the co-culture assay design with $TGFB2^{+/+}$ and $TGFB2^{KO/+}$ CPC-SMCs. (D) Relative SMC marker levels in the following conditions: $TGFB2^{+/+}$ CPC-SMCs co-cultured with $TGFB2^{+/+}$ CPC-SMCs (black columns); $TGFB2^{KO/+}$ CPC-SMCs co-cultured with $TGFB2^{KO/+}$ CPC-SMCs (red columns) and $TGFB2^{KO/+}$ CPC-SMCs co-cultured with $TGFB2^{+/+}$ CPC-SMCs (gray columns). $n = 6$ biological replicates. ns: not significant; 1-way ANOVA with multiple comparisons test. (E) Relative SMC marker levels in $TGFB2^{KO/+}$ CPC-SMCs supplemented with either active TGFB2 or vehicle for 7 days during CPC-SMC differentiation. The average expression in vehicle samples was set to 1. $n = 6$ biological replicates. ns: not significant; unpaired t-test or Mann-Whitney U test. (F) Relative SMC marker levels in $TGFB2^{+/+}$ CPC-SMCs treated with 1ug/mL TGFB2 neutralization antibody. The average expression in the control samples was set to 1. $n = 6$ biological replicates. ns: not significant; unpaired t-test.

2 ng/mL TGFB2 for 7 days during the standard CPC-SMC differentiation with TGFB1. Consistently, SMC marker expression was significantly improved in $TGFB2^{KO/+}$ CPC-SMCs after TGFB2 supplementation (Figure 4E). Lastly, we blocked TGFB2 activity in our culture system using a neutralizing TGFB2 antibody.[50] To accomplish this, we supplemented the culture medium with the neutralizing TGFB2 antibody during the differentiation of $TGFB2^{+/+}$ CPC-SMCs (Figure 4F). TGFB2 neutralization significantly reduced the expression of several SMC markers suggesting that SMC-produced TGFB2 contributes to CPC-SMC differentiation (Figure 4F).

TGFBR3$^{KO/KO}$ causes reduced TGFB2 sensitivity in *TGFB2*$^{KO/+}$ SMCs

To further investigate the interplay between TGFB2 and TGFBR3, we used *TGFB2*$^{KO/+}$ hiPSCs, and generated 2 independent clones of *TGFB2*$^{KO/+}$*TGFBR3*$^{KO/KO}$ using CRISPR/Cas9 gene editing. The Clone 1 had a 14 base-pair bi-allelic deletion and the Clone 2 had 1 base-pair bi-allelic insertion in *TGFBR3* gene resulting in premature stop codons in exon 9 of *TGFBR3* gene (Figure 5A). Both clones had more than 1000-folds reduction in *TGFBR3* expression (Figure 5B). Next, we differentiated *TGFB2*$^{KO/+}$, *TGFB2*$^{KO/+}$*TGFBR3*$^{KO/KO}$, and their isogenic control hiPSCs (*TGFB2*$^{+/+}$*TGFBR3*$^{+/+}$) to CPC-SMCs using active TGFB2 (Figure 5C). As expected, SMC differentiation with active TGFB2 effectively rescued SMC marker expression in *TGFB2*$^{KO/+}$ CPC-SMCs (Figure 5C). Strikingly, the marker expression in *TGFB2*$^{KO/+}$*TGFBR3*$^{KO/KO}$ CPC-SMCs did not recover during TGFB2-mediated differentiation further implicating the TGFBR3 dependence in TGFB2 mediated signal transduction (Figure 5C).

We also assessed the functional defects caused by TGFB2 and TGFBR3 deficiencies using 3D tissue ring constructs.[51,52] To generate the tissue rings, *TGFB2*$^{KO/+}$, *TGFB2*$^{KO/+}$*TGFBR3*$^{KO/KO}$, and their isogenic control CPC-SMCs were differentiated with active TGFB2 and seeded around 2 mm agarose molds. The rings were supplemented for 2 weeks with TGFB2 instead of TGFB1. To understand the molecular and cellular defects, we performed immunofluorescence stainings to assess SMC organization and contractile protein levels in the tissue ring constructs. MYH11 staining intensity and SMC distribution were improved in the *TGFB2*$^{KO/+}$ rings generated with TGFB2, similar to the isogenic control rings (Figure 5D). MYH11 stainings of *TGFB2*$^{KO/+}$*TGFBR3*$^{KO/KO}$ tissue rings from both clones revealed significantly weaker MYH11 staining intensity (Figure 5D and E). MYH11+ cells in the control and the *TGFB2*$^{KO/+}$ rings had elongated morphology while they had uncharacteristic round shape for SMCs in the *TGFB2*$^{KO/+}$*TGFBR3*$^{KO/KO}$ rings (Figure 5D). The cell density was also unaffected by *TGFBR3*$^{KO/KO}$ (Figure 5E) suggesting defective SMC differentiation in the presence of TGFB2 as the underlying cause for the ring defects.

TGFB2^{G276R} variant disrupts the mechanical properties of vascular tissue rings

Lastly, we identified a family with heritable cardiovascular disorders for 3 generations of aortic aneurysm and dissection at Michigan Medicine. The Clinical Genetic testing revealed that the 54-year old male family member with aortic root aneurysm (root diameter: 5.2 cm) carries a variant in *TGFB2* gene (c.826G > A; Chr1: 218436041 [GRCh38]; rs1169804851; ClinVar accession: VCV001450986; allele frequency = 0.000011 [3/264690, TOPMED]) and did not carry any variants in the remaining aortopathy panel genes. This *TGFB2* variant causes a single amino acid substitution nearby the furin cleavage site in the latency-associated peptide domain of TGFB2 protein (p.Gly276Arg). To examine G276R substitution in the same isogenic background, we generated hiPSCs using the peripheral blood mononuclear cells of the male patient carrying the variant (*Patient*$^{G276R/+}$), and corrected the mutation in the hiPSCs (*Patient*$^{+/+}$) using CRISPR/Cas9 gene editing (Figure 6A). *TGFB2* expression in *Patient*$^{G276R/+}$ and *Patient*$^{+/+}$ CPC-SMCs were similar while TGFB2 ELISA on cell lysates indicated lower TGFB2 protein levels in the *Patient*$^{G276R/+}$ (Figure S3A). Cycloheximide chase assay showed a higher TGFB2 degradation rate in *Patient*$^{G276R/+}$ cells compared to *Patient*$^{+/+}$ cells suggesting reduced stability of TGFB2 p.Gly276Arg (Figure S3B). The transwell co-culture assays revealed that *Patient*$^{+/+}$ CPC-SMCs have higher expression of SMC markers including *MYH11*, *CNN1,* and *SMTN* (Figure S3C). Similarly, *Patient*$^{G276R/+}$ CPC-SMCs co-cultured with *Patient*$^{+/+}$ CPC-SMCs had higher SMC marker expression (Figure S3C). We also treated *Patient*$^{G276R/+}$ and *Patient*$^{+/+}$ CPC-SMCs with vehicle or 2 ng/mL TGFB2 for 7 days during the standard CPC-SMC differentiation with TGFB1. As expected, SMC markers including *MYH11*, *CNN1,* and *SMTN* were upregulated in *Patient*$^{G276R/+}$ CPC-SMCs after TGFB2 treatment (Figure S3D), while *Patient*$^{+/+}$ CPC-SMCs did not appear to respond to the TGFB2 treatment (Figure S3E).

Next, we assessed the functional defects caused by the p.Gly276Arg substitution using the tissue ring model. TGFB2 ELISA without the acidification step confirmed the elevated active TGFB2 levels in the *Patient*$^{+/+}$ tissue rings (Figure S3F). The tensile strength of the rings was improved in the *Patient*$^{+/+}$ constructs (Figure 6B). TGFB2 supplementation during the tissue ring formation also improved the mechanical properties of *Patient*$^{G276R/+}$ tissue rings (Figure 6B). Immunostainings revealed increased MYH11 intensity in the *Patient*$^{+/+}$ tissue rings and the TGFB2-supplemented *Patient*$^{G276R/+}$ rings, while the cell density was unchanged across different conditions (Figure 6C and D, Figure S4). To confirm this finding in an independent genetic background, we used hiPSCs (*TGFB2*$^{+/+}$) from a male donor with no aortic abnormalities and generated hiPSCs carrying c.826G > A mutation (*TGFB2*$^{G276R/+}$) by CRISPR/Cas9 gene editing (Figure 6E). The mutant *TGFB2*$^{G276R/+}$ tissue rings had significantly lower tensile strength compared with the isogenic *TGFB2*$^{+/+}$ tissue rings (Figure 6F). TGFB2 supplementation of the *TGFB2*$^{G276R/+}$ rings improved the tensile strength (Figure 6F). Consistent with the *Patient*$^{G276R/+}$ tissue ring data, immunostainings showed reduced MYH11 staining intensity and uncharacteristic round cell morphology in the *TGFB2*$^{G276R/+}$ rings compared to the isogenic control *TGFB2*$^{+/+}$ and TGFB2 supplemented *TGFB2*$^{G276R/+}$ rings (Figure 6G and H, Figure S5). The cell density was unaffected by the p.Gly276Arg substitution suggesting defective SMC differentiation as the primary culprit for the mechanical and molecular changes (Figure 6H).

Discussion

Here we used hiPSC-derived SMC differentiation, CRISPR/Cas9 gene editing, SMC tissue constructs, and human tissue specimens to gain mechanistic insights into TGFB2-related aortopathy. Despite the similarities between the biological activities of different TGFβ isoforms in hiPSC-derived SMC differentiation, we found that TGFB2 additionally requires TGFBR3 to exert its effects on SMC gene expression. The molecular evaluation of different human thoracic aorta segments suggested *TGFB2* and *TGFBR3* enrichment in the aortic root. We found that *TGFB2* haploinsufficiency causes second heart field-derived SMC differentiation defects that can be rescued by TGFB2 supplementation. This is in line with the findings from the *Tgfb2* haploinsufficiency mouse model, which has aortic root dilation.[7] *TGFBR3*^{KO} prevented the molecular rescue of *TGFB2* haploinsufficiency with TGFB2 supplementation suggesting the TGFBR3 dependence in TGFB2 mediated

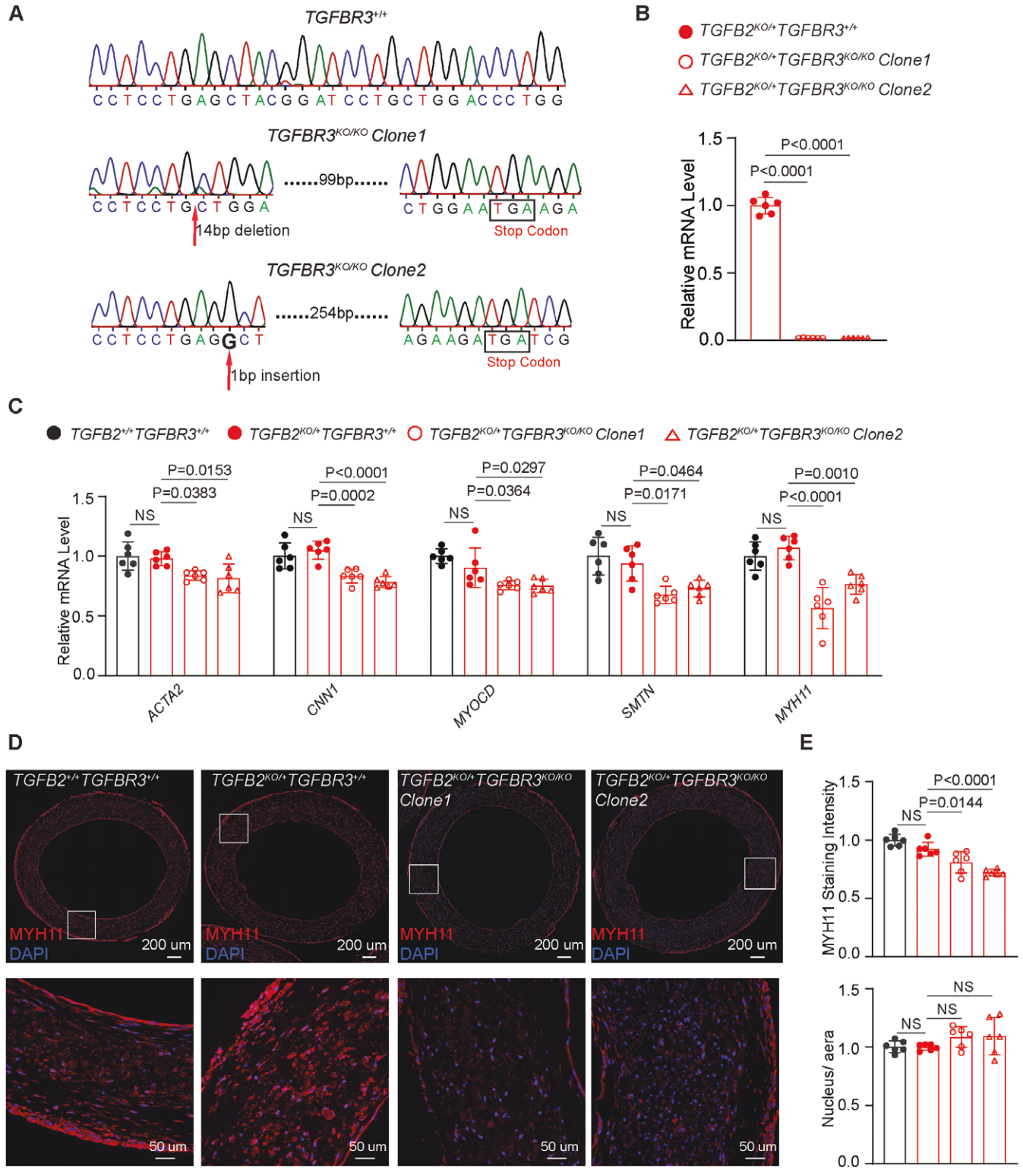

Figure 5. *TGFBR3*$^{KO/KO}$ causes reduced TGFB2 sensitivity in *TGFB2*$^{KO/+}$ SMCs. (A) The Sanger sequencing results showing 2 independent *TGFBR3*$^{KO/KO}$ hiPSC clones with premature *TGFBR3* stop codons generated by CRISPR/Cas9 gene editing. (B) Relative *TGFBR3* expression in different conditions. $n = 6$ biological replicates; 1-way ANOVA with multiple comparisons test. (C) Relative SMC marker expression in *TGFB2*$^{KO/+}$, 2 *TGFB2*$^{KO/+}$*TGFBR3*$^{KO/KO}$ clones and isogenic control (*TGFB2*$^{+/+}$*TGFBR3*$^{+/+}$) CPC-SMCs differentiated with TGFB2. $n = 6$ biological replicates; ns: not significant; 1-way ANOVA with multiple comparisons test. (D-E) MYH11 staining intensity and cell density in *TGFB2*$^{KO/+}$, *TGFB2*$^{KO/+}$*TGFBR3*$^{KO/KO}$, and isogenic control (*TGFB2*$^{+/+}$*TGFBR3*$^{+/+}$) tissue rings generated using TGFB2. The average values in *TGFB2*$^{+/+}$*TGFBR3*$^{+/+}$ rings were set to 1. $n = 6$ biological replicates; ns: not significant; 1-way ANOVA with multiple comparisons test.

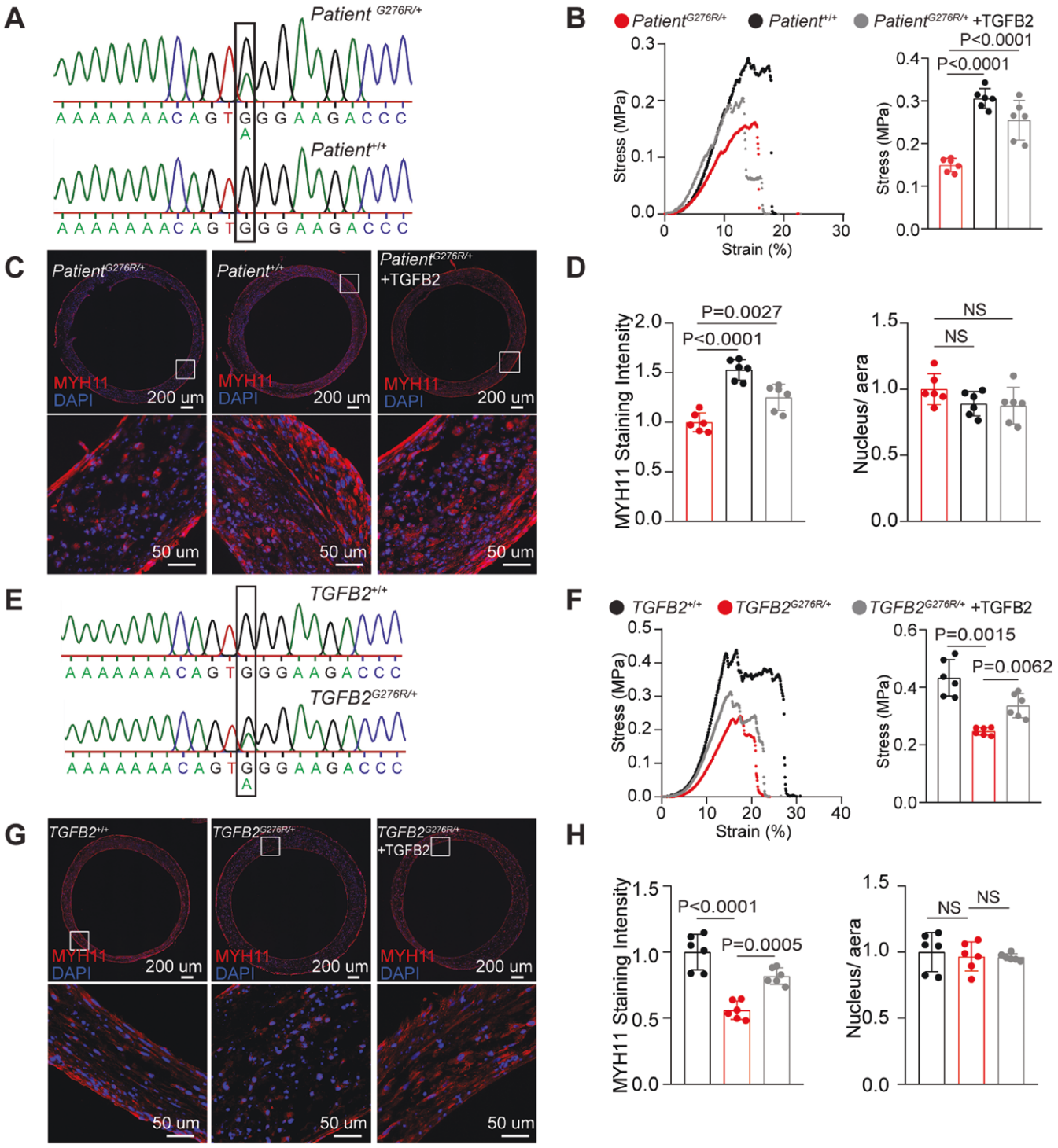

Figure 6. *TGFB2*^{G276R} variant disrupts the mechanical properties of vascular tissue rings. (A) The Sanger sequencing results showing the position of c.826G > A variant and its CRISPR/Cas9-based genetic correction (black rectangle). (B) Representative stress-strain curves and maximum tensile stress values from *Patient*$^{G276R/+}$, *Patient*$^{+/+}$ tissue rings as well as *Patient*$^{G276R/+}$ rings treated with TGFB2. $n = 6$ biological replicates; 1-way ANOVA with multiple comparisons test. (C-D) MYH11 staining intensity and cell density in *Patient*$^{G276R/+}$, *Patient*$^{+/+}$ tissue rings as well as *Patient*$^{G276R/+}$ rings supplemented with TGFB2. The average values in *Patient*$^{G276R/+}$ samples were set to 1. $n = 6$ biological replicates; ns: not significant; 1-way ANOVA with multiple comparisons test. (E) The Sanger sequencing results for *TGFB2*$^{+/+}$ and *TGFB2*$^{G276R/+}$ hiPSCs. (F) Representative stress-strain curves and maximum tensile stress values from *TGFB2*$^{+/+}$, *TGFB2*$^{G276R/+}$ as well as *TGFB2*$^{G276R/+}$ tissue rings treated with TGFB2. $n = 6$ biological replicates; 1-way ANOVA with multiple comparisons test. (G-H) MYH11 staining intensity and cell density in *TGFB2*$^{+/+}$, *TGFB2*$^{G276R/+}$ as well as *TGFB2*$^{G276R/+}$ tissue rings supplemented with TGFB2. The average values in *Patient*$^{G276R/+}$ samples were set to 1. $n = 6$ biological replicates; ns: not significant; 1-way ANOVA with multiple comparisons test.

SMC differentiation. SiRNA experiments were also in support of this finding. Our data also suggests that missense variant (c.826G > A, p.Gly276Arg) in *TGFB2* gene causes mechanical and cellular deficits in the 3D tissue ring constructs, which can be rescued by CRISPR/Cas9-based genetic correction and TGFB2 supplementation. As this missense variant is located near the furin cleavage site, we speculate that it may impair the proteolytical activation of TGFB2, reducing activated TGFB2 levels in our culture conditions. In sum, this study reveals the regional TGFB2 expression patterns in the human thoracic aorta and its reliance on TGFBR3 in CPC-SMC differentiation, defects which could contribute to aortic root aneurysm formation.

There are 3 TGFβ isoforms identified in mammalian tissues; TGFB1, TGFB2, and TGFB3.[53] Although pathogenic variants in *TGFB2* and *TGFB3* genes have been associated with LDS, there are no known pathogenic *TGFB1* variants linked to the disease. Genetic disruption of different TGFβ isoforms in mice has non-overlapping features with *Tgfb2* deficiency causing congenital heart defects and distinct cardiovascular abnormalities such as aortic wall thinning.[20,26,54] *Tgfb2* is highly expressed in the aortic valves and aortic annulus in the developing mouse heart and MacFarlane et al. demonstrated TGFB2 enrichment in the mouse aortic root compared with ascending aorta.[15,55] Our analysis of tunica media from different thoracic aorta regions revealed both *TGFB2* and *TGFBR3* enrichment in the human aortic root. The distinct TGFB2 expression pattern likely contributes to its nonredundant activity in cardiovascular development and the association between pathogenic *TGFB2* variants and aortic root aneurysms. Additionally, we found that CPC-SMC differentiation is sensitive to TGFB2 supplementation and speculate that lineage-driven SMC sensitivity to TGFβ isoforms can also contribute to regional aortic aneurysm presentations in patients carrying pathogenic TGFβ signaling variants.

TGFBR3 is a critical but understudied member of TGFβ signaling. It has a high affinity for TGFB2 and promotes signaling via TGFBR1-TGFBR2 receptor complex by facilitating TGFβ ligand presentation.[47] Pathogenic *TGFBR3* variants have been associated with intracranial aneurysms.[56] Similar to the unique phenotypic characteristics in *Tgfb2* knockout mice, *Tgfbr3* deficient embryos exhibit defects in outflow tract, heart valves, and coronary arteries, and comparative analyses of *Tgfbr3* and *Tgfb2* knockout embryos point to overlapping roles of these genes in heart development.[57,58] Our data indicate that TGFB2 requires TGFBR3 to activate downstream TGFβ signaling during SMC differentiation. This distinct mode of action suggests that the interplay between TGFBR3 and TGFB2 should be better characterized in the context of aortic root aneurysms.

Patients with pathogenic *TGFB2* variants exhibit milder TAAD and systemic phenotypes distinguishable from those seen in patients carrying *TGFBR1*, *TGFBR2*, or *SMAD3* variants.[7,30] Our comparative analysis indicates that different TGFβ isoforms display similar biological effects on hiPSC-derived SMC differentiation. Although *TGFB2* shows enrichment in the aortic root, the other TGFβ isoforms are also expressed in this part of the aorta. We predict that the redundant activities of different TGFβ isoforms can compensate for TGFB2 defects resulting in relatively later onset and milder aggressiveness of pathogenic *TGFB2* variants. In addition, a compensatory increase in the expression of TGFβ isoforms was reported in human aortas from patients with Marfan Syndrome or pathogenic TGFB2 variants implying additional transcriptional regulation to offset the defects.[7,31,59]

Summary

This study posits TGFB2 as a physiologically relevant cue for SMC differentiation in human aortic root, its reliance on TGFBR3 for signal transduction, and provides mechanistic implications about the TAAD manifestations in patients with TGFB2 defects.

Author contributions

Y.T.: Conceptualization, Data curation, Formal analysis, Investigation, Methodology, Validation, Visualization, Writing—original draft, review and editing. J.C.: Data curation, Investigation, Validation. C.H.: Data curation, Investigation, Validation. P.Q.: Conceptualization, Methodology. J.L.: Data curation, Investigation, Validation. Y.E.C.: Conceptualization, Funding acquisition. D.M.: Conceptualization, Methodology, Writing—original draft, review and editing, Funding acquisition, Supervision, Visualization. B.Y.: Conceptualization, Resources, Writing—review and editing, Funding acquisition, Supervision, Visualization.

Funding

This study was supported by National Institutes of Health grants HL130614, HL141891, and HL151776 (B.Y.), and HL109946, HL134569, and HL159871 (Y.E.C.). D.M. is supported by MI-AORTA Rapid Research and Frankel Cardiovascular Center Aortic Research Grants.

Conflicts of interest

The authors have declared no potential conflicts of interest.

Data availability

The data that support the findings of this study are available from the corresponding authors upon reasonable request.

Supplementary material

Supplementary material is available at *Stem Cells Translational Medicine* online.

References

1. Isselbacher EM, Lino Cardenas CL, Lindsay ME. Hereditary influence in thoracic aortic aneurysm and dissection. *Circulation*. 2016;133:2516-2528. https://doi.org/10.1161/CIRCULATIONAHA.116.009762
2. Pinard A, Jones GT, Milewicz DM. Genetics of thoracic and abdominal aortic diseases. *Circ Res*. 2019;124:588-606. https://doi.org/10.1161/CIRCRESAHA.118.312436
3. Isselbacher EM. Thoracic and abdominal aortic aneurysms. *Circulation*. 2005;111:816-828. https://doi.org/10.1161/01.CIR.0000154569.08857.7A
4. Meester JAN, Verstraeten A, Schepers D, et al. Differences in manifestations of Marfan syndrome, Ehlers-Danlos syndrome, and Loeys-Dietz syndrome. *Ann Cardiothorac Surg*. 2017;6:582-594. https://doi.org/10.21037/acs.2017.11.03

5. Loeys BL, Schwarze U, Holm T, et al. Aneurysm syndromes caused by mutations in the TGF-beta receptor. *N Engl J Med*. 2006;355:788-798. https://doi.org/10.1056/NEJMoa055695
6. Bertoli-Avella AM, Gillis E, Morisaki H, et al. Mutations in a TGF-beta ligand, TGFB3, cause syndromic aortic aneurysms and dissections. *J Am Coll Cardiol*. 2015;65:1324-1336. https://doi.org/10.1016/j.jacc.2015.01.040
7. Lindsay ME, Schepers D, Bolar NA, et al. Loss-of-function mutations in TGFB2 cause a syndromic presentation of thoracic aortic aneurysm. *Nat Genet*. 2012;44:922-927. https://doi.org/10.1038/ng.2349
8. Cardoso S, Robertson SP, Daniel PB. TGFBR1 mutations associated with Loeys-Dietz syndrome are inactivating. *J Recept Signal Transduct Res*. 2012;32:150-155. https://doi.org/10.3109/10799893.2012.664553
9. Dawson A, Li Y, Li Y, et al. Single-cell analysis of aneurysmal aortic tissue in patients with Marfan syndrome reveals dysfunctional TGF-beta signaling. *Genes (Basel)* 2021;13:95. https://doi.org/10.3390/genes13010095
10. Gillis E, Van Laer L, Loeys BL. Genetics of thoracic aortic aneurysm: at the crossroad of transforming growth factor-beta signaling and vascular smooth muscle cell contractility. *Circ Res*. 2013;113:327-340. https://doi.org/10.1161/CIRCRESAHA.113.300675
11. Inamoto S, Kwartler CS, Lafont AL, et al. TGFBR2 mutations alter smooth muscle cell phenotype and predispose to thoracic aortic aneurysms and dissections. *Cardiovasc Res*. 2010;88:520-529. https://doi.org/10.1093/cvr/cvq230
12. Milewicz DM, Guo D-C, Tran-Fadulu V, et al. Genetic basis of thoracic aortic aneurysms and dissections: focus on smooth muscle cell contractile dysfunction. *Annu Rev Genomics Hum Genet*. 2008;9:283-302. https://doi.org/10.1146/annurev.genom.8.080706.092303
13. Micha D, Guo DC, Hilhorst-Hofstee Y, et al. SMAD2 mutations are associated with arterial aneurysms and dissections. *Hum Mutat*. 2015;36:1145-1149. https://doi.org/10.1002/humu.22854
14. van de Laar IMBH, Oldenburg RA, Pals G, et al. Mutations in SMAD3 cause a syndromic form of aortic aneurysms and dissections with early-onset osteoarthritis. *Nat Genet*. 2011;43:121-126. https://doi.org/10.1038/ng.744
15. MacFarlane EG, Parker SJ, Shin JY, et al. Lineage-specific events underlie aortic root aneurysm pathogenesis in Loeys-Dietz syndrome. *J Clin Invest*. 2019;129:659-675. https://doi.org/10.1172/JCI123547
16. Zhou D, Feng H, Yang Y, et al. hiPSC Modeling of lineage-specific smooth muscle cell defects caused by *TGFBR1A230T* variant, and its therapeutic implications for Loeys-Dietz Syndrome. *Circulation*. 2021;144:1145-1159. https://doi.org/10.1161/CIRCULATIONAHA.121.054744
17. Hu JH, Wei H, Jaffe M, et al. Postnatal deletion of the Type II transforming growth factor-beta receptor in smooth muscle cells causes severe aortopathy in mice. *Arterioscler Thromb Vasc Biol*. 2015;35:2647-2656. https://doi.org/10.1161/ATVBAHA.115.306573
18. Zhang YE. Non-smad signaling pathways of the TGF-beta family. *Cold Spring Harb Perspect Biol*. 2017;9(2):a022129. https://doi.org/10.1101/cshperspect.a022129
19. Doetschman T, Barnett JV, Runyan RB, et al. Transforming growth factor beta signaling in adult cardiovascular diseases and repair. *Cell Tissue Res*. 2012;347:203-223. https://doi.org/10.1007/s00441-011-1241-3
20. Sanford LP, Ormsby I, Gittenberger-de Groot AC, et al. TGFbeta2 knockout mice have multiple developmental defects that are non-overlapping with other TGFbeta knockout phenotypes. *Development*. 1997;124:2659-2670. https://doi.org/10.1242/dev.124.13.2659
21. Diebold RJ, Eis MJ, Yin M, et al. Early-onset multifocal inflammation in the transforming growth factor beta 1-null mouse is lymphocyte mediated. *Proc Natl Acad Sci U S A*. 1995;92:12215-12219. https://doi.org/10.1073/pnas.92.26.12215
22. Kulkarni AB, Huh CG, Becker D, et al. Transforming growth factor beta 1 null mutation in mice causes excessive inflammatory response and early death. *Proc Natl Acad Sci U S A*. 1993;90:770-774. https://doi.org/10.1073/pnas.90.2.770
23. Shull MM, Ormsby I, Kier AB, et al. Targeted disruption of the mouse transforming growth factor-beta 1 gene results in multifocal inflammatory disease. *Nature*. 1992;359:693-699. https://doi.org/10.1038/359693a0
24. Kaartinen V, Voncken JW, Shuler C, et al. Abnormal lung development and cleft palate in mice lacking TGF-beta 3 indicates defects of epithelial-mesenchymal interaction. *Nat Genet*. 1995;11:415-421. https://doi.org/10.1038/ng1295-415
25. Proetzel G, Pawlowski SA, Wiles MV, et al. Transforming growth factor-beta 3 is required for secondary palate fusion. *Nat Genet*. 1995;11:409-414. https://doi.org/10.1038/ng1295-409
26. Molin DG, DeRuiter MC, Wisse LJ, et al. Altered apoptosis pattern during pharyngeal arch artery remodelling is associated with aortic arch malformations in Tgfbeta2 knock-out mice. *Cardiovasc Res*. 2002;56:312-322. https://doi.org/10.1016/s0008-6363(02)00542-4
27. Azhar M, Brown K, Gard C, et al. Transforming growth factor Beta2 is required for valve remodeling during heart development. *Dev Dyn*. 2011;240:2127-2141. https://doi.org/10.1002/dvdy.22702
28. Bartram U, Molin DG, Wisse LJ, et al. Double-outlet right ventricle and overriding tricuspid valve reflect disturbances of looping, myocardialization, endocardial cushion differentiation, and apoptosis in TGF-beta(2)-knockout mice. *Circulation*. 2001;103:2745-2752. https://doi.org/10.1161/01.cir.103.22.2745
29. Molin DG, Bartram U, Van der Heiden K, et al. Expression patterns of Tgfbeta1-3 associate with myocardialisation of the outflow tract and the development of the epicardium and the fibrous heart skeleton. *Dev Dyn*. 2003;227:431-444. https://doi.org/10.1002/dvdy.10314
30. Schepers D, Tortora G, Morisaki H, et al. A mutation update on the LDS-associated genes TGFB2/3 and SMAD2/3. *Hum Mutat*. 2018;39:621-634. https://doi.org/10.1002/humu.23407
31. Boileau C, Guo DC, Hanna N, et al; National Heart, Lung, and Blood Institute (NHLBI) Go Exome Sequencing Project. TGFB2 mutations cause familial thoracic aortic aneurysms and dissections associated with mild systemic features of Marfan syndrome. *Nat Genet*. 2012;44:916-921. https://doi.org/10.1038/ng.2348
32. Kinoshita A, Saito T, Tomita H, et al. Domain-specific mutations in TGFB1 result in Camurati-Engelmann disease. *Nat Genet*. 2000;26:19-20. https://doi.org/10.1038/79128
33. Shimizu C, Jain S, Davila S, et al. Transforming growth factor-beta signaling pathway in patients with Kawasaki disease. *Circ Cardiovasc Genet*. 2011;4:16-25. https://doi.org/10.1161/CIRCGENETICS.110.940858
34. Gong J, Zhou D, Jiang L, et al. In vitro lineage-specific differentiation of vascular smooth muscle cells in response to SMAD3 deficiency: implications for SMAD3-related thoracic aortic aneurysm. *Arterioscler Thromb Vasc Biol*. 2020;40:1651-1663. https://doi.org/10.1161/ATVBAHA.120.313033
35. Cao N, Liang H, Huang J, et al. Highly efficient induction and long-term maintenance of multipotent cardiovascular progenitors from human pluripotent stem cells under defined conditions. *Cell Res*. 2013;23:1119-1132. https://doi.org/10.1038/cr.2013.102
36. Hu J, Wang Y, Jiao J, et al. Patient-specific cardiovascular progenitor cells derived from integration-free induced pluripotent stem cells for vascular tissue regeneration. *Biomaterials*. 2015;73:51-59. https://doi.org/10.1016/j.biomaterials.2015.09.008
37. Wang A, Tang Z, Li X, et al. Derivation of smooth muscle cells with neural crest origin from human induced pluripotent stem cells. *Cells Tissues Organs*. 2012;195:5-14. https://doi.org/10.1159/000331412
38. Patsch C, Challet-Meylan L, Thoma EC, et al. Generation of vascular endothelial and smooth muscle cells from human pluripotent

stem cells. *Nat Cell Biol*. 2015;17:994-1003. https://doi.org/10.1038/ncb3205
39. Dash BC, Levi K, Schwan J, et al. Tissue-engineered vascular rings from human iPSC-derived smooth muscle cells. *Stem Cell Rep*. 2016;7:19-28. https://doi.org/10.1016/j.stemcr.2016.05.004
40. Trempolec N, Degavre C, Doix B, et al. Acidosis-induced TGF-beta2 production promotes lipid droplet formation in dendritic cells and alters their potential to support anti-mesothelioma T cell response. *Cancers (Basel)* 2020;12:1284. https://doi.org/10.3390/cancers12051284
41. Oida T, Weiner HL. Depletion of TGF-beta from fetal bovine serum. *J Immunol Methods*. 2010;362:195-198. https://doi.org/10.1016/j.jim.2010.09.008
42. Schneider CA, Rasband WS, Eliceiri KW. NIH Image to ImageJ: 25 years of image analysis. *Nat Methods*. 2012;9:671-675. https://doi.org/10.1038/nmeth.2089
43. Majesky MW. Developmental basis of vascular smooth muscle diversity. *Arterioscler Thromb Vasc Biol*. 2007;27:1248-1258. https://doi.org/10.1161/ATVBAHA.107.141069
44. Sawada H, Rateri DL, Moorleghen JJ, Majesky MW, Daugherty A. Smooth muscle cells derived from second heart field and cardiac neural crest reside in spatially distinct domains in the media of the ascending aorta-brief report. *Arterioscler Thromb Vasc Biol*. 2017;37:1722-1726. https://doi.org/10.1161/ATVBAHA.117.309599
45. Shen M, Quertermous T, Fischbein MP, Wu JC. Generation of vascular smooth muscle cells from induced pluripotent stem cells: methods, applications, and considerations. *Circ Res*. 2021;128:670-686. https://doi.org/10.1161/CIRCRESAHA.120.318049
46. Sun T, Huang Z, Liang WC, et al. TGFbeta2 and TGFbeta3 isoforms drive fibrotic disease pathogenesis. *Sci Transl Med*. 2021;13(605):eabe0407. https://doi.org/10.1126/scitranslmed.abe0407
47. Villarreal MM, Kim SK, Barron L, et al. Binding properties of the transforming growth factor-beta coreceptor betaglycan: proposed mechanism for potentiation of receptor complex assembly and signaling. *Biochemistry*. 2016;55:6880-6896. https://doi.org/10.1021/acs.biochem.6b00566
48. Vander Ark A, Cao J, Li X. TGF-beta receptors: in and beyond TGF-beta signaling. *Cell Signal*. 2018;52:112-120. https://doi.org/10.1016/j.cellsig.2018.09.002
49. Xie WB, Li Z, Shi N, et al. Smad2 and myocardin-related transcription factor B cooperatively regulate vascular smooth muscle differentiation from neural crest cells. *Circ Res*. 2013;113:e76-e86. https://doi.org/10.1161/CIRCRESAHA.113.301921
50. Lu JM, Song XJ, Wang HF, Li X-L, Zhang X-R. Murine corneal stroma cells inhibit LPS-induced dendritic cell maturation partially through TGF-beta2 secretion in vitro. *Mol Vis*. 2012;18:2255-2264.
51. Gwyther TA, Hu JZ, Billiar KL, Rolle MW. Directed cellular self-assembly to fabricate cell-derived tissue rings for biomechanical analysis and tissue engineering. *J Vis Exp*. 2011;(57):e3366. https://doi.org/10.3791/3366
52. Gwyther TA, Hu JZ, Christakis AG, et al. Engineered vascular tissue fabricated from aggregated smooth muscle cells. *Cells Tissues Organs*. 2011;194:13-24. https://doi.org/10.1159/000322554
53. Morikawa M, Derynck R, Miyazono K. TGF-beta and the TGF-beta family: context-dependent roles in cell and tissue physiology. *Cold Spring Harb Perspect Biol*. 2016;8:a021873. https://doi.org/10.1101/cshperspect.a021873
54. Azhar M, Schultz Jel J, Grupp I, et al. Transforming growth factor beta in cardiovascular development and function. *Cytokine Growth Factor Rev*. 2003;14:391-407.
55. Snider P, Standley KN, Wang J, et al. Origin of cardiac fibroblasts and the role of periostin. *Circ Res*. 2009;105:934-947. https://doi.org/10.1161/CIRCRESAHA.109.201400
56. Santiago-Sim T, Mathew-Joseph S, Pannu H, et al. Sequencing of TGF-beta pathway genes in familial cases of intracranial aneurysm. *Stroke*. 2009;40:1604-1611. https://doi.org/10.1161/STROKEAHA.108.540245
57. Compton LA, Potash DA, Brown CB, Barnett JV. Coronary vessel development is dependent on the type III transforming growth factor beta receptor. *Circ Res*. 2007;101:784-791. https://doi.org/10.1161/CIRCRESAHA.107.152082
58. Stenvers KL, Tursky ML, Harder KW, et al. Heart and liver defects and reduced transforming growth factor beta2 sensitivity in transforming growth factor beta type III receptor-deficient embryos. *Mol Cell Biol*. 2003;23:4371-4385. https://doi.org/10.1128/MCB.23.12.4371-4385.2003
59. Nataatmadja M, West J, West M. Overexpression of transforming growth factor-beta is associated with increased hyaluronan content and impairment of repair in Marfan syndrome aortic aneurysm. *Circulation*. 2006;114:I371-I377. https://doi.org/10.1161/CIRCULATIONAHA.105.000927